



# Water Resistance, Biodegradation and Thermal Stability of Thermoplastic Starch Reinforced with Unvulcanized Natural Rubber, Epoxidized Natural Rubber and Dissolving Pulp

Yeiangchart Boonluksiri<sup>1</sup> · Phoempon Siangdang<sup>1</sup> · Yeampon Nakaramontri<sup>1</sup>

Accepted: 17 October 2022 / Published online: 1 November 2022

© The Author(s), under exclusive licence to Springer Science+Business Media, LLC, part of Springer Nature 2022

## Abstract

Biodegradable thermoplastic starch (TPS) has been expected to be sustainable alternative to petrochemical-based polymers due to its biodegradability with proper and controlled costs. However, brittleness and biodegradation rate of TPS are insufficient for usage as a single material. The present work aims to improve TPS properties by incorporating with unvulcanized natural rubber (NR), epoxidized NR with 25 and 50 mol% epoxide (ENR25 and ENR50) and 0–15 phr of dissolving pulp (Fiber) using combined techniques of internal mixer and compression molding at 180 °C. The results based on mechanical properties, water resistance, biodegradation and thermal stability of TPS were studied. It was found that the tensile properties, following ASTM D638 Type I, increased after the addition of ENR25 relative to the NR and ENR50 cases. In addition, the combination of 10 wt% ENR50 and 15 phr fiber to the TPS showed high potential on improvement of tensile properties of the composites relating polarity effects. This blending ratios also enhanced the thermal stability of the composites, relating the thermogravimetric analyzer (TGA), whereas the solubility and disintegration in terms of the dimensions and shape of the TPS after water and soil exposure were reduced monitoring through weight loss investigation. This means that the incorporation of ENR50 and fiber at 10 wt% and 15 phr, respectively, to the TPS properly showed a synergistic effect on increasing of TPS properties by increasing flexibility and retarding biodegradation rate after soil exposure for 60 days. This environmentally friendly materials could be use as seed tray, slow released fertilizer for agriculture applications.

**Keywords** Thermoplastic starch · Natural rubber · Dissolving pulp · Stability · Biodegradation · Hydrolysis

## Introduction

Thermoplastic starch (TPS) is a biodegradable polymer based on renewable resources made from plasticized starch. Due to its rapid biodegradability and low cost, TPS is expected to be a sustainable alternative to petrochemical-based polymers and a solution for solving environmental problems. This made TPS for fabricating in several key potential applications including packaging, agricultural and biomedical products. Unfortunately, the insufficient mechanical characteristics and low stability of TPS limit its applications. The main limitations of TPS are brittleness,

moisture sensitivity and hydrophilicity, resulting in low dimensional stability and fast degradation during usage. To improve the mechanical properties of TPS, modification, blending or reinforcement with other polymers or materials are required [1].

The moisture sensitivity of TPS greatly affects its mechanical characteristics and stability. Blending TPS with hydrophobic polymers is one of the effective technique to reduce the hydrophilicity and brittleness of the TPS. Hydrophobic polymers, including petroleum-based polymers, biopolymers, or elastomers, have been reported to enhance the mechanical characteristics and stability of TPS [2–4], in particular the natural rubber (NR) which is one of the most flexible elastomers. NR has numerous excellent physical characteristics, including hydrophobic, high flexibility, minimal heat build-up, and great fatigue resistance [5]. In addition, the modified form of NR, so-called epoxidized NR (ENR), has excellent elasticity, toughness, strength and oil resistance. The epoxy groups by means of the epoxirane ring

✉ Yeampon Nakaramontri  
yeampon.nak@kmutt.ac.th

<sup>1</sup> Sustainable Polymer and Innovative Composite Materials Research Group, Department of Chemistry, Faculty of Science, King Mongkut's University of Technology Thonburi (KMUTT), Thungkru, Bangkok 10140, Thailand

in ENR molecular structure effectively cause the polarity on ENR backbone and this improves its compatibility to the other polar polymers [6]. Thus, compatibilization degree of ENR depends on the degree of epoxidation, which is available in two commercial grades i.e., ENR with 25 and 50 mol% epoxidation (ENR-25 and ENR-50) [7]. The ductility and water resistance properties of the TPS can increase by blending with epoxidized natural rubber. This enhanced the mechanical properties in terms of elongation at break and decreased water absorption percentage. These effects are controlled by the degree of polymer compatibility and water resistance [8]. Effect of polarity for increasing compatibility among rubber and TPS molecules was also studied by using the oxidized NR (ONR), resulting in improved hydrophobicity and brittleness of the blends [8]. With requirement of existing polar functional groups on the chains, applying ENR and chitosan powder was also reported. It was found that the incorporation of chitosan improved mechanical and dynamical properties of the blends and the ENR showed well performance for interacting to TPS [4, 9]. However, this phenomenon can be changed, depending on degree of polarity, such as the oxirane ring on ENR molecules. with TPS than NR [4].

The reinforcement with organic fibers has also been reported to improve the mechanical properties of TPS [10]. Lignocellulose fiber contains naturally cellulosic materials, including cellulose, hemicellulose, and lignin, and has been used as a reinforcing fiber in TPS. The incorporation of such fibers improved the tensile strength and modulus but decreased the moisture resistance of the TPS/cellulose composite [11]. The addition of cellulose considerably increased the mechanical properties of TPS/fiber composites due to compatibility with the decreasing lignin percentage [12]. The fiber of the dissolving pulp had a cellulose percentage higher than 90% and a low lignin content. Moreover, cellulose nanofibers increased thermal stability and delayed the degradation of starch nanocomposites [13].

Although the addition of unmodified and modified NR, as the ENR, for enhancing the mechanical properties, water resistance and/or thermal stability of the TPS were individually reported following several researchers as mentioned earlier [4, 6, 8, 10–12], the development of TPS incorporated with both of unvulcanized NR and fiber has not been prior reported. Therefore, the present work aims to investigate the effect of a combined use of unvulcanized NR and ENR with dissolving pulp fiber on mechanical properties, thermal stability, water resistance and biodegradation of TPS. The optimal content of dissolving pulp fiber and types of unvulcanized rubber to improve those properties of TPS composites were explored. Also, biodegradation mechanism of the composites was illustrated. Development of TPS composites could improve the usability and expand applications of the environmental friendliness material.

## Materials and Methods

### Materials and Chemicals

Thermoplastic starch (TPS; TAPIOPLAST®TPS FC) manufactured from tapioca starch plasticized with vegetable oil at a density of  $1.8 \text{ g cm}^{-2}$  was purchased from Siam Modified Starch Co., Ltd., Pathum Thani, Thailand. Natural rubber (NR; STR 5L) was provided by Nabon Rubber Co., Ltd., Nakhon Si Thammarat, Thailand. Epoxidized natural rubber with 25 mol% epoxide (ENR25; Epoxyrene 25) and 50 mol% epoxide (ENR50; Epoxyrene 50) were obtained from Muang Mai Guthrie Public Co., Ltd., Surat Thani, Thailand. Natural fiber as a polymeric fiber reinforcement (dissolving pulp; PPPC Diamond grade) at an approximate alpha-cellulose of 95.5% was supplied by SCG Packaging Co., Ltd., Bangkok, Thailand.

### Specimen Preparation

TPS was pre-dried in a hot air oven at  $60 \text{ }^\circ\text{C}$  for at least 24 h before individually blended with NR, ENR25 or ENR50. TPS/rubber blends containing 0, 5, 10, 15, 20 and 25 wt% of rubber contents were prepared before mixing with dissolving pulp (Fiber) at contents varying from 0, 5, 10 and 15 phr. The blends and composites were mixed by using an internal mixer (CT MX75; Chareon tut Co., Ltd., Samutprakarn, Thailand) at mixing temperature of  $180 \text{ }^\circ\text{C}$  with a rotor speed of 60 rpm for the total mixing operation of approximately 10 min. The TPS/rubber and TPS/rubber/fiber were formed by a compression molding machine (LP-20 M; Labtech Engineering, Thailand) at  $180 \text{ }^\circ\text{C}$  for 10 min and then cooled down for 5 min (Fig. 1). Specimens for tensile testing and phase morphology observation were formed in dumbbell-shaped (Type I) following standard testing method of ASTM D638 with thickness of 3.2 mm. In addition, specimen sheets for thermal stability and biodegradation measurements were cut into  $20 \times 30 \text{ mm}^2$  with a thickness of 1 mm before the testing. Formulation of TPS composite is shown in Table 1.

### Material Characterization & Testing

#### Effects of Unvulcanized Rubber and Fiber on Mechanical Properties of TPS

**Mechanical Properties** Tensile properties of TPS composites were tested according to the standard testing method of ASTM D638 (Type I) by using a universal testing machine (Autograph AG-I; Shimadzu, Japan). The tests were performed with a crosshead speed of  $5 \text{ mm min}^{-1}$  at room tem-

**Fig. 1** Compression molding equipment with separated hot and cooling zones

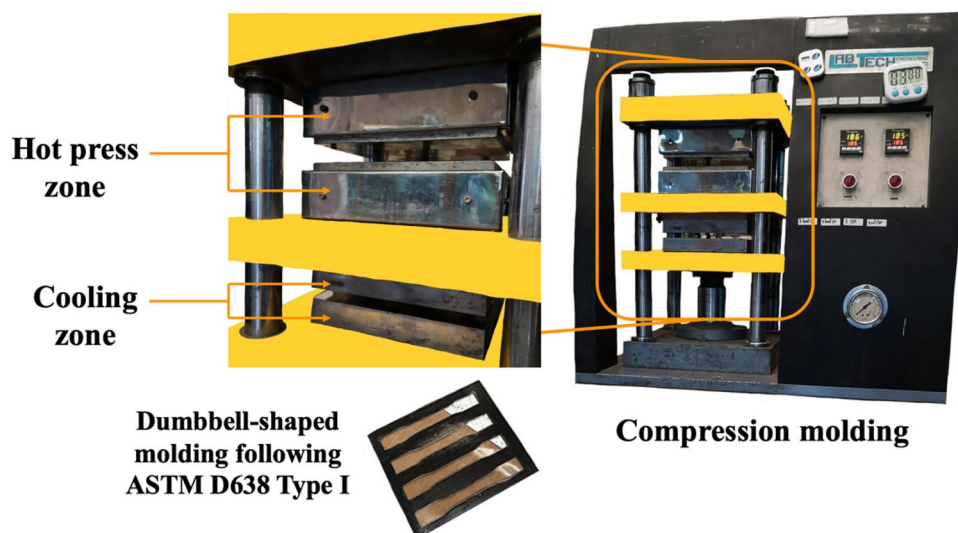


**Table 1** Formulations of TPS composites incorporated with NR, ENR and Fiber

Sample codes	TPS (wt%)	NR (wt%)	ENR25 (wt%)	ENR50 (wt%)	Fiber (phr)
TPS/NR-10	90	10	–	–	–
TPS/E25-10	90	–	10	–	–
TPS/E50-10	90	–	–	10	–
TPS/NR-10/F15	90	10	–	–	15
TPS/E25-10/F15	90	–	10	–	15
TPS/E50-10/F15	90	–	–	10	15
TPS/NR-20	80	20	–	–	–
TPS/E25-20	80	–	20	–	–
TPS/E50-20	80	–	–	20	–
TPS/NR-20/F15	80	20	–	–	15
TPS/E25-20/F15	80	–	20	–	15
TPS/E50-20/F15	80	–	–	20	15

perature. The tensile properties of the blends and composites were determined in terms of tensile strength, elongation at break and tensile modulus. The average value of at least five replicates was reported.

**Phase Morphology** TPS blends and composites were fractured under liquid nitrogen for sharp and smooth surface before sputter coating with gold. Cross-sections morphologies of the fractured specimens were evaluated using scanning electron microscope (SEM; JSM-6610LV, JEOL Ltd., Tokyo, Japan) with 1000× magnification at accelerated voltage of 10 kV.

#### Effect of Unvulcanized ENR and Fiber on Thermal Stability of TPS

**Thermal Stability** Thermal stability was determined using thermogravimetric analyzer (TGA; STA 8000, PerkinElmer, Inc., Massachusetts, USA). The samples were placed in the

desiccator with silica gel for at least 24 h to remove moisture, then taken in ceramic pan and heated from 30 to 600 °C with a heating rate of 10 °C min<sup>-1</sup>. The results were reported in terms of mass loss percentage and the derivative mass loss as a function of temperature.

**Elemental Composition** The samples were placed in the desiccator with silica gel for at least 24 h for removing moisture. Elemental composition of TPS, TPS/E50 and TPS/E50/Fiber were determined using elemental analyzer (CHNS/O analyzer; 628 series, Leco Corp., St. Joseph, MI, USA) following the standard method of ASTM-D5373. The total carbon, hydrogen, nitrogen, sulphur and oxygen percentages were reported. In addition, the higher heating value (HHV) of each sample was calculated following the Eq. (1) and reported:

$$\text{HHV} (\text{MJkg}^{-1}) = 0.344\text{C} + \text{H} + 0.105\text{S} - (0.106\text{O} + 0.015\text{N}) \quad (1)$$

where the C, H, S, O and N are the carbon, hydrogen, sulphur, oxygen and nitrogen percentages, respectively. It is noted that the coefficients of the C, H, S, O and N are 0.344, 1.000, 0.105, 0.106 and 0.015, respectively [12].

### Effect of Unvulcanized ENR and Fiber on Biodegradation of TPS

**Degradation Under Submerged Condition** Degradation under submerged condition of TPS, TPS/E50 and TPS/E50/Fiber specimens were tested at mesophilic temperature ( $30 \pm 2$  °C). The specimens were immersed in 20 ml of distilled water before collecting for weight monitoring. The results were reported in terms of percentages of swelling degree, dissolving, and weight loss. Percentage of swelling degree was calculated following Eq. (2), measuring the wet weight gained of the specimens:

$$\text{Degree of swelling (\%)} = \frac{W_{\text{swell}} - W_{\text{initial}}}{W_{\text{initial}}} \times 100 \quad (2)$$

where the  $W_{\text{initial}}$  and  $W_{\text{swell}}$  refer to the specimen weights before and after swelling test, respectively. The percentages of dissolving and weight loss were calculated through Eq. (3) following the dried weight of specimens.

$$\text{Weight loss(\%)} = \frac{W_{\text{initial}} - W_{\text{final}}}{W_{\text{initial}}} \times 100 \quad (3)$$

where  $W_{\text{initial}}$  and  $W_{\text{final}}$  are specimen weight before and after degradation test, respectively.

**Degradation Under Soil Burial** Aerobic biodegradation under soil burial of TPS, TPS/E50 and TPS/E50/fiber were performed at mesophilic temperature ( $30 \pm 2$  °C). Soil mixtures were prepared by mixing agricultural soil with plant compost at a ratio of 25:1 respectively. Physical and chemical properties of soil was presented in Table 2. The soil was sampling to find moisture percentage via moisture balance analyzer, then the soil moisture was calculated and adjusted to approximately 45% by distilled water. Then, the specimen sheets were buried in a container of prepared soil for 60 days. The sheets were collected for monitoring weight

**Table 2** Physical and chemical properties of soil using in the tests

Physiochemical properties of soil	Value
pH (1:1 w/v H <sub>2</sub> O)	7.60
Organic matter (%)	3.64
Total organic carbon (%)	2.11
Total organic nitrogen (%)	0.14
C/N ratio	15.07

every 15 days, and reported the weight loss percentage following Eq. (3).

## Results and Discussion

### Effects of Unvulcanized Rubber and Fiber on Mechanical Properties of TPS

The effects of the unvulcanized rubber types and their fiber contents on the mechanical properties of TPS, including the tensile strength, elongation at break, and tensile modulus, are shown in Fig. 2. TPS was blended with NR, ENR25 or ENR50 at contents of 0, 5, 10, 15, 20 and 25 wt%. Tensile strength and elongation at break of TPS/ENR25 and TPS/ENR50 blends increased higher than those of the TPS/NR blends, especially TPS with the addition of ENR25 and ENR50 at contents of 20 and 10 wt%, respectively. ENR has a greater effect on the tensile strength and elongation at break of TPS than NR due to blend compatibility enhancement from the chemical interaction between the epoxy group of ENR and the hydroxyl group of TPS may form covalent bonding [14], which is stronger than a weak interfacial interaction of NR/TPS [4, 15, 16]. The correlated explanation was reported also by Cai et al. and Pichaiyut et al. [4, 14]. That is, the addition of ENR25 increased tensile strength and elongation at break of the intrinsic TPS in the higher level of the use of ENR50 regarding chemical interaction among polar functional groups of ENR and TPS molecular chains and also lower the capability for strain-induced crystallization of the rubber [17, 18]. This is well agreement to the reports of Jaratrotkamjorn et al. relating new formation of the ENR-TPS linkages [19].

Additionally, the optimal rubber content formed a continuous phase in the TPS blends, but excess rubber content destroyed the strong intermolecular interactions and entanglement between the molecular chains of TPS by replacement with rubber, resulting in decreasing the tensile strength of TPS [4, 20]. Conversely, the tensile modulus of TPS/NR was much higher than that of TPS/ENR25 and TPS/ENR50 because the tensile modulus of TPS is low, and the addition of NR enhanced this characteristic [21]. The addition of NR affected the tensile modulus more than the addition of ENR due to the compatibility, flexibility, and low elastic modulus of ENR [9, 22]. Therefore, the uses of NR, ENR25 and ENR50 at 10 and 20 wt% were selected for blending with TPS in order to study the effects of the unvulcanized rubber and fiber on properties of the blend composites.

In order to study the effects of unvulcanized rubber types and fiber contents on the tensile properties of TPS. The TPS was individually blended with NR, ENR25 or ENR50 at contents of 10 and 20 wt%, then mixed with fiber at 0, 5, 10 and 15 phr. The results of tensile strength, elongation at

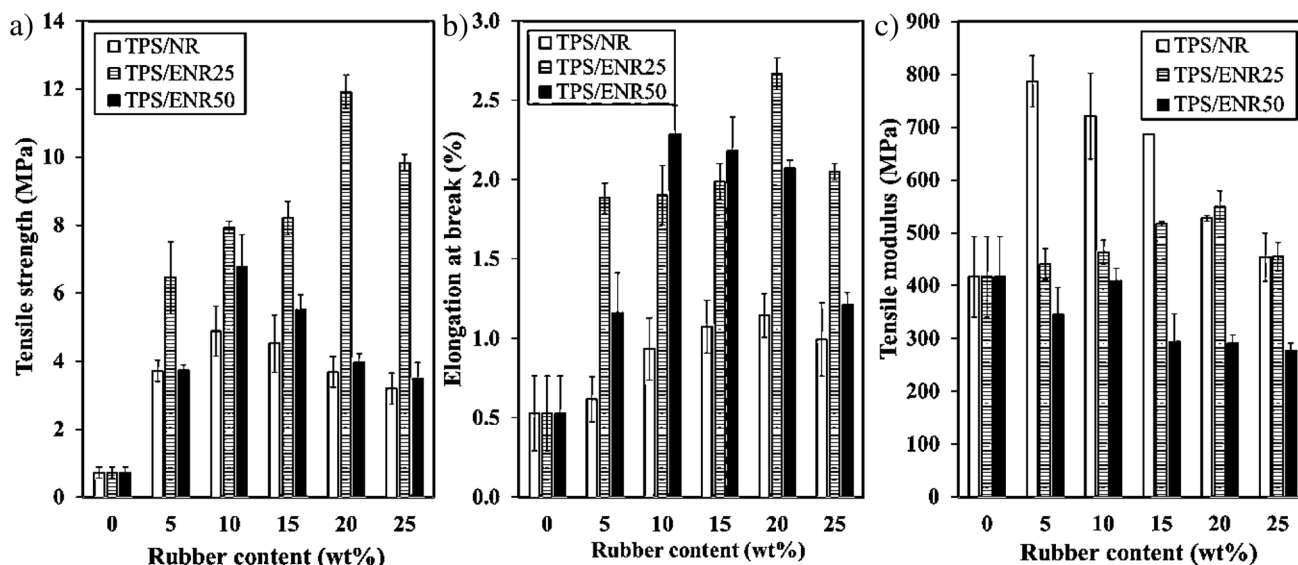


**Fig. 2** Tensile properties of TPS/rubber blends: **a** tensile strength, **b** elongation at break, and **c** tensile modulus

break and tensile modulus are shown in Fig. 3. It was found that tensile strength and tensile modulus of TPS/NR, TPS/ENR25 and TPS/ENR50 with the addition of fiber increased with increasing fiber content, but the elongation at break slightly changed. This can be explained that the interaction between fiber and TPS matrix, which formed a strong adhesion through dipole–dipole intermolecular improved the tensile strength of TPS. Besides, the rigidity and immobilization characteristics of the fiber restrained the molecular chain mobility and free volume of TPS forces, corresponded with Kaewtatip and Thongmee and Fahrngruber et al. [23, 24].

The combined use of unvulcanized rubbers and fiber showed a synergistic effect on tensile properties of the TPS composites, especially at 10 wt% of rubber addition. The effect of fiber content on mechanical properties of TPS composites with 10 wt% of added rubber was more pronounced than in the composites with 20 wt%. This indicated that the rubber loadings and types impacted the brittleness of the TPS due to the formation of a continuous phase of rubber. In addition, tensile strength and elongation at break of the TPS/ENR/fiber composite were greater than those of the TPS/NR/fiber composite since polar epoxy group of ENR has dipole-dipole interfacial interaction with TPS, whereas NR (non-polar) has no interaction with polar amylose and amylopectin in starch structure [4, 15, 16]. In addition, the highest tensile strength, elongation at break and tensile modulus of TPS composite was found in the TPS/E50-10/F15 composite. This is attributed to the high polarity of the ENR50, which has a greater opportunity to act as a binder between the TPS molecular chains and the fiber surfaces. It not only provided a strong covalent bond between the epoxy

group of ENR and the hydroxyl groups of the TPS and the fiber but also ample hydrogen bonding between the starch and cellulose [25, 26]. The similar explanation was also reported by Saetun et al. and Jiang et al.

In order to verify the effect of unvulcanized rubbers and fiber formation, the surface fracture morphologies of TPS/rubber blends and TPS/rubber/fiber composites were investigated. Figure 4 shows the phase morphologies of TPS/NR, TPS/ENR25, and TPS/ENR50 with and without added fiber imaged with a scanning electron microscope (SEM). The dark phases represent the TPS matrix, the brighter phases represent the rubber domains, and the brightest phases represent the fiber. Adding NR without fiber induced microcracking in the TPS due to phase separation, immiscibility, and poor adhesion between the NR and the TPS [21]. Conversely, the addition of ENR without fiber tended to blend with TPS better than the NR addition by forming a co-continuous morphology. This occurred due to the high hydrophilicity and polarity of ENR; the chemical interaction between the polar functional groups of TPS and ENR enhanced compatibility [14]. After adding the fiber to TPS/rubber, the rubber domains became smaller, randomly agglomerated with the fiber, and were simultaneously distributed in the TPS matrix. This can be explained that hydrogen bonding between epoxy groups of ENR and hydroxyl groups of cellulose served as physical cross-linking network, which improved interfacial adhesion and uniform dispersion corresponded with Cao et al. [27].

Conversely, adding fiber to TPS/ENR25 and TPS/ENR50 induced microcracking from the phase separation of TPS and fiber. The oxirane ring of ENR was the limiting factor for simultaneous compatibilization with TPS

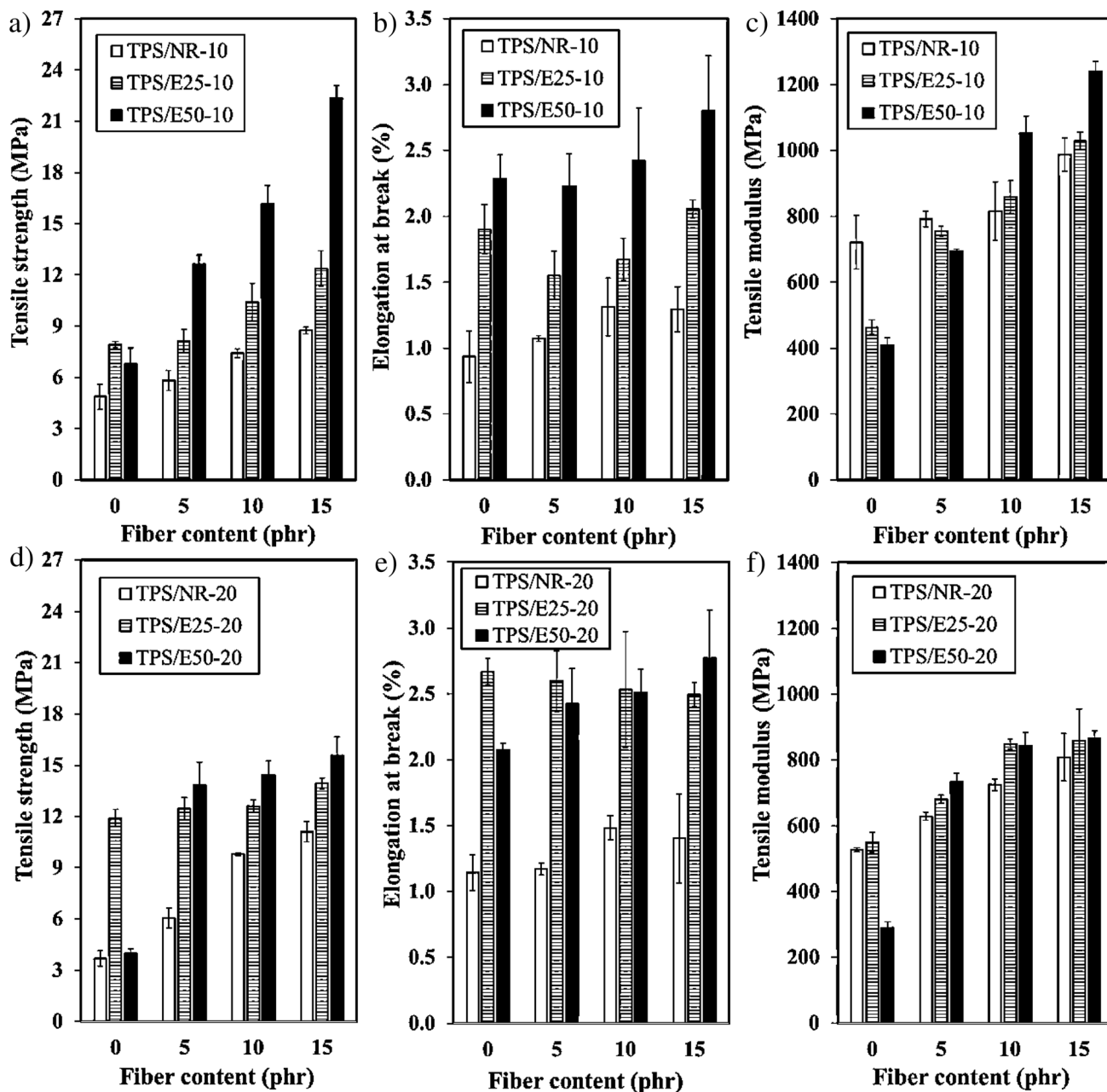


**Fig. 3** Tensile properties by means of tensile strength, elongation at break and tensile modulus of TPS/rubber blends filled with various fiber contents of 0–15 phr, while the images a–c are assigned to rubber loading 10% and images d–f are 20%

and fiber. Any excess cellulose provided phase separation and weak interfacial adhesion from agglomeration [4, 28]. Therefore, the combined use of 10 wt% ENR50 and 15 phr fiber efficiently reinforced the mechanical properties of TPS. Thus, the TPS/ENR50/fiber composite was selected as the representative sample for the material degradation experiments.

### Effect of Unvulcanized ENR and Fiber on Thermal Stability of TPS

TPS with a combination of 10 wt % ENR50 and 15 phr fiber (TPS/ENR50/fiber) was selected as the representative for the material degradation experiments. The thermal degradation of TPS, TPS/ENR50, and TPS/ENR50/fiber

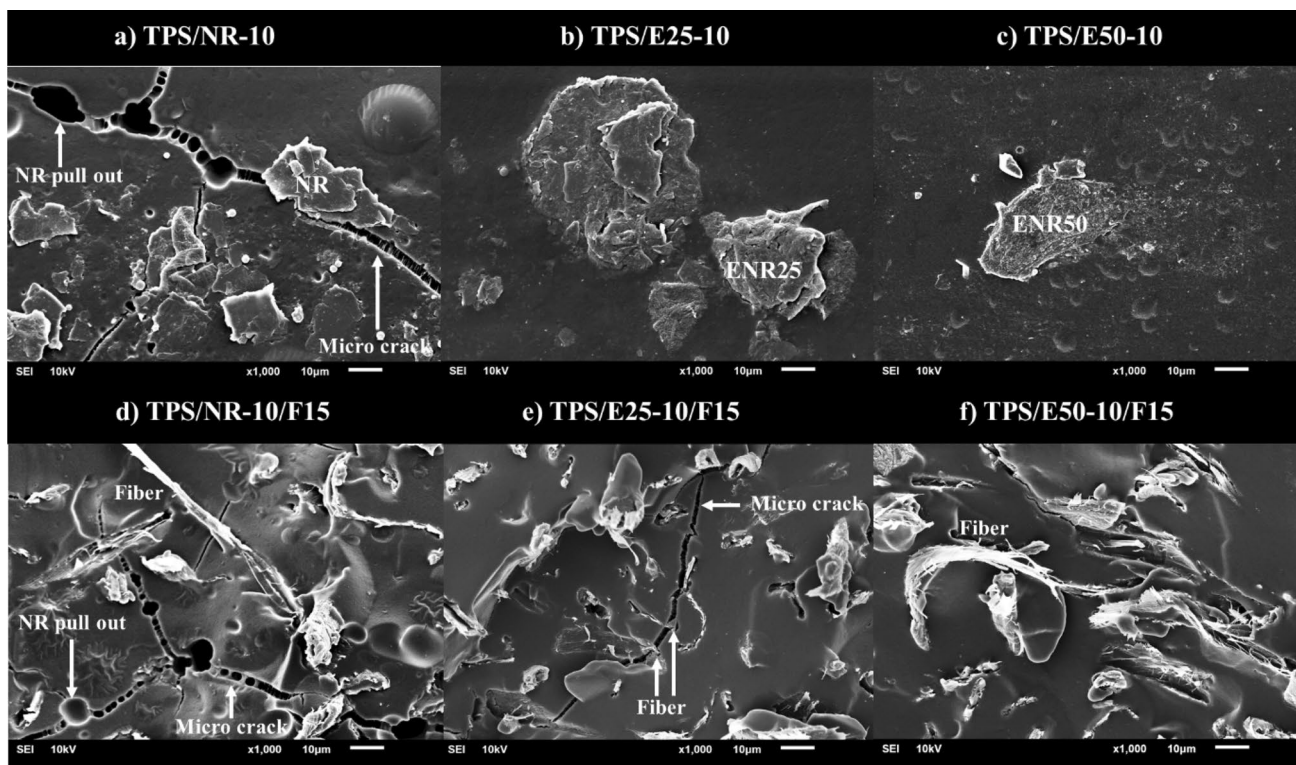


**Fig. 4** SEM images of TPS composites: **a** TPS/NR-10, **b** TPS/E25-10, **c** TPS/E50-10, **d** TPS/NR-10/F15, **e** TPS/E25-10/F15, and **f** TPS/E50-10/F15

was determined using a thermogravimetric analyzer heated from 30 to 600 °C with a heating rate of 10 °C min<sup>-1</sup>. Thermal stability through the TGA and DTG thermograms is reported in Fig. 5. The TGA thermogram exhibited three major degradation steps resulting in different temperatures, as seen in Fig. 5a. The received onset degradation temperatures of TPS, fiber, and ENR50 were 299.91, 343.51 and 367.96 °C, respectively. Degradation temperature of TPS improved with the addition of both ENR50 and fiber due to the chemical interactions of polar functional groups in TPS and oxirane groups in ENR50, and hydrogen bonding between fiber and TPS. In addition, Fig. 5b shows the DTG thermogram which exhibited three decomposition temperatures of TPS, fiber, and ENR50 were 319.00, 361.17, and 399.67 °C, respectively. The addition of ENR50 dramatically decreased the derivative mass loss of the TPS at 319 °C, and exhibited peak intensity of ENR50 decomposition temperature at 399.67 °C. Meanwhile, the addition of fiber slightly improved the thermal stability of TPS/ENR50, indicating that the added ENR50 affected the thermal stability of TPS more than the addition of both ENR50 and fiber because the decomposition temperature and interfacial chemical interaction of ENR influenced the thermal resistance of the blends [29, 30] more than the interfacial dipole–dipole interaction of cellulose.

Based on the presented degree of decomposition, the changes in the elemental analysis were also used to confirm the effects of element composition on the thermal stability of the TPS blends. The total carbon (C), hydrogen (H), nitrogen (N), sulfur (S), oxygen (O), and higher heating values (HHV) are reported in Table 3. The addition of ENR50 with TPS increased the percentage of carbon and the HHV of TPS. In addition, the incorporation of fiber slightly increased the percentage of carbon and the HHV of TPS/ENR50 due to the high carbon and hydrogen content of the rubber, which enhanced the C/O ratio of the blend, and the carbon content increased the energy density of the cellulose, resulting in higher thermal stability [31, 32]. Based on Fig. 5b and Table 3, the addition of ENR50 and ENR50/Fiber increased thermal stability of the composites relating appearance of carbon elements. This affirms well the improvement of the thermal resistance of TPS blended with ENR and ENR/Fiber.

### Effect of Unvulcanized ENR and Fiber on Biodegradation of TPS

The degradability of the TPS composites was examined using swelling and burying tests. Thus, the degradation under submerged conditions of the TPS, TPS/E50, and TPS/

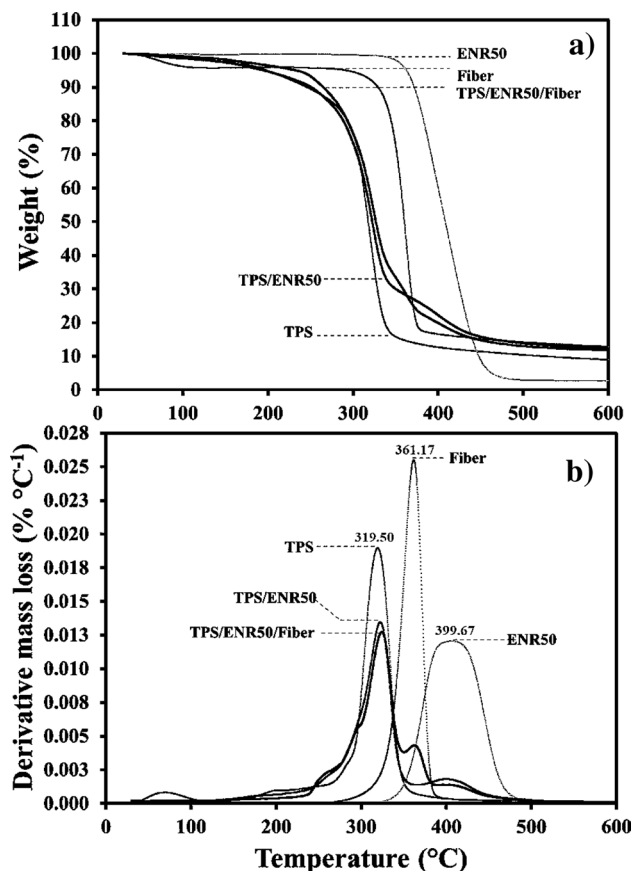


**Fig. 5** Thermogravimetry analysis curve of TPS, TPS/ENR50 blend and TPS/ENR50/Fiber composite: **a** weight percentage and **b** derivative mass loss percentage

E50/fiber composites was tested at mesophilic temperature ( $30 \pm 2$  °C) by immersing the samples in 20 ml of distilled water for at least 80 min. The correlations between the swelling and dissolving degrees are presented in terms of weight gain and weight loss. Figure 6 shows the degree of swelling of the blends. The observed swelling degree of the pristine TPS increased and then disintegrated after immersion for 40 min. Also, the swellability of the TPS with added ENR50 disintegrated after immersion for 80 min, indicating that the additional ENR50 retarded the degradation of TPS. Disintegration of composites was due to the diminishing effect of the hydrophobicity of rubber on the polarity of the

TPS backbone and the hindering of the hydrogen bonding between the TPS and water [33].

Interestingly, disintegration during the swelling test of the TPS/ENR50/fiber composite was not observed after immersion for 80 min, as seen in the images in Fig. 7. The dimensions and shape of the TPS/ENR50/Fiber sheets were still acceptable, but the sheets were no longer transparent but white following the swelling test. In contrast, the sheets of TPS/ENR50 without added fiber lost both their transparency and shape. This is generally attributed to the voids between the interphase of the hydrophilic TPS and hydrophobic rubber, which allowed water absorption [34, 35], resulting in the rapid whitening of the blend. Unfortunately, the pristine TPS sheets without ENR50 and fiber disintegrated into small pieces from mass loss during the swelling test. This disintegration was faster than that of the composites containing any additions due to the hydrophilic nature of TPS. The formation of hydrogen bonding between the free hydrogen group of the TPS and water led to the fast water uptake of TPS, which dissolved after saturation [36]. The similar phenomenon was also explained by Abdul Wahab et al. relating the biodegradable rate of the blends composites [36].

The solubility of the TPS, TPS/E50, and TPS/E50/fiber composites in terms of dissolving percentage is shown in Fig. 8. The specimens were immersed in distilled water for 80 min before drying. The percentage of dissolution of pristine TPS, TPS/ENR50, and TPS/E50/fiber increased with increased immersion time; first, the pristine TPS, followed by the TPS with the addition of ENR50 and fiber. Conversely, the dissolvability of ENR50 did not change, but the sheets lost their shape (Fig. 9). The TPS and TPS/ENR50 sheets without fiber broke into fragments and shrank due to the solubility of the TPS but the TPS/ENR50 with added fiber only deformed. This difference is because there are fewer active sites for water absorption due to the strong interactions between the hydroxyl groups of cellulose and TPS. Besides, the molecular chain mobility of the TPS was restricted by the strong chemical interaction between the polymer and the reinforcements [37, 38], leading to the increased shape stability of TPS. The finding was also reported previously by Ghanbari which indicated that the blending of TPS retards well decomposition of the composites [38].

**Table 3** Element composition of the C, N, O, S, N and the HHV of TPS, TPS/ENR50 blend and TPS/ENR50/Fiber composite

Sample	Elemental analysis (%)					HHV (MJ/kg)
	C	H	N	S	O	
ENR50	74.97 ± 0.06	12.04 ± 0.01	1.63 ± 0.04	0.00	11.35 ± 0.02	39.90 ± 0.04
Fiber	41.05 ± 0.19	7.50 ± 0.15	1.73 ± 0.42	0.00	49.72 ± 0.76	15.43 ± 0.42
TPS	38.56 ± 0.89	7.76 ± 0.15	1.07 ± 0.03	0.00	52.61 ± 1.02	14.46 ± 0.69
TPS/ENR50	42.03 ± 0.09	7.99 ± 0.06	0.95 ± 0.12	0.00	49.02 ± 0.02	16.58 ± 0.11
TPS/ENR50/Fiber	43.01 ± 1.19	7.78 ± 0.47	0.12 ± 0.00	0.00	49.10 ± 0.72	16.59 ± 0.14

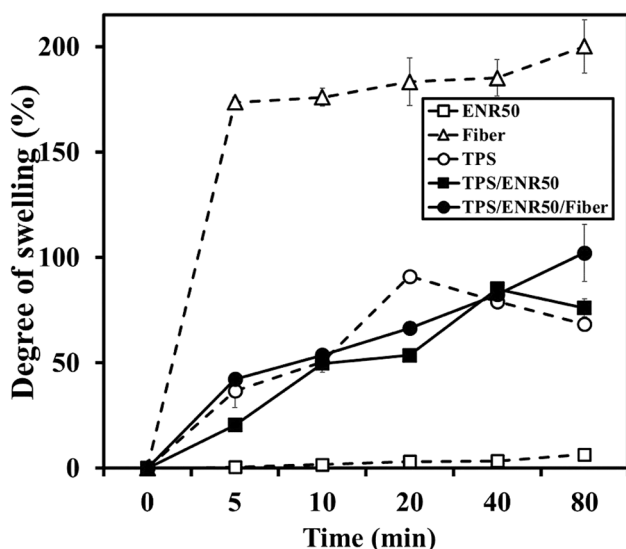


**Fig. 6** Swelling degree of TPS, TPS/ENR50 blend and TPS/ENR50/Fiber composites

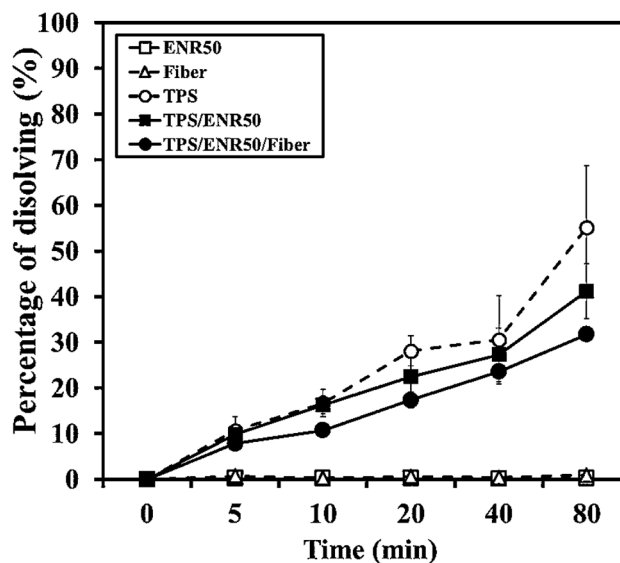


**Fig. 8** Percentage of dissolving of TPS, TPS/ENR50 blend and TPS/ENR50/Fiber composites

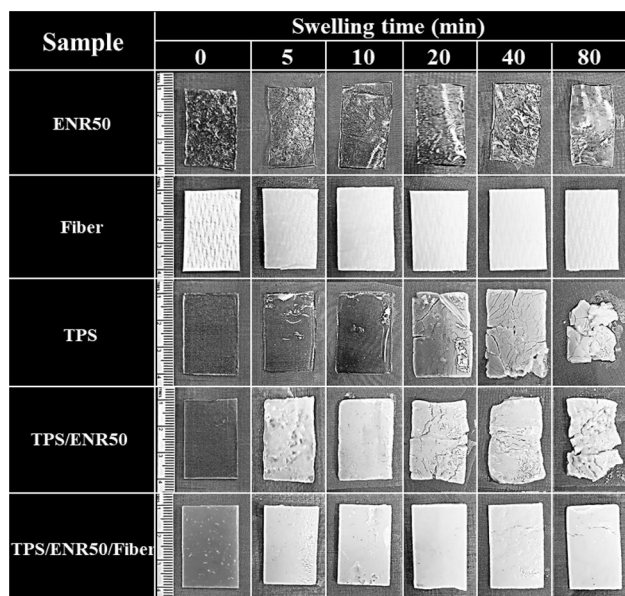


**Fig. 7** Appearance of the composites after swelling test of TPS, TPS/ENR50 blend and TPS/ENR50/Fiber

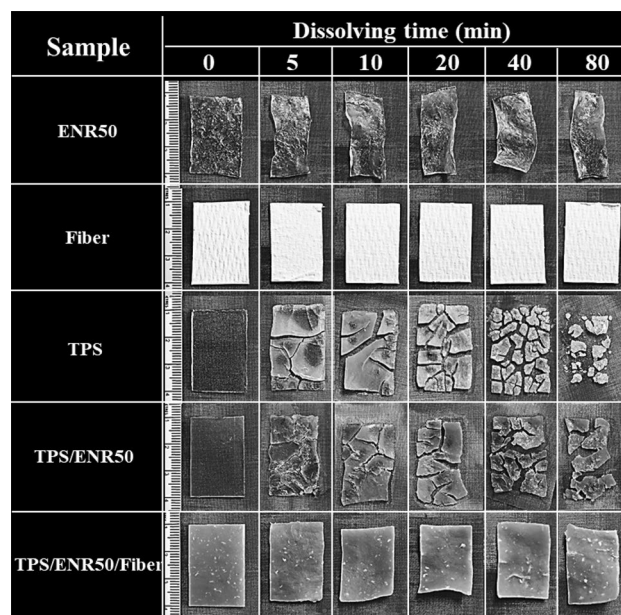


**Fig. 9** Appearance of the composites after solubility test of TPS, TPS/ENR50 blend and TPS/ENR50/Fiber

The biodegradation results for TPS, TPS/ENR50, and TPS/ENR50/fiber in terms of the percentage of the sheet weight loss after exposure to water and soil at mesophilic temperature ( $30 \pm 2$  °C) for 60 days are shown in Fig. 10. The sheet weight loss percentage under water dramatically increased in the first 15 days of hydrolysis, then slightly changed (Fig. 10a). The addition of ENR50/fiber decreased the hydrolysis of TPS, resulting in a lower sheet weight loss percentage than that of TPS/ENR50, followed by the pristine TPS. This loss relates to the intermolecular interaction

between the epoxy group of the ENR and the hydroxyl group of the limited reactive sites of TPS starch that interact with water [39]. Therefore, the insolubility of ENR and cellulose fiber limited the solubilizing ability of TPS, leading to the lower hydrolysis rates of the blend.

Furthermore, the biodegradation of TPS after burial in soil is reported in Fig. 10b. The highest percentage of TPS weight loss was almost 80% within 60 days. The weight loss percentage of TPS, TPS/ENR50, and TPS/ENR50/fiber

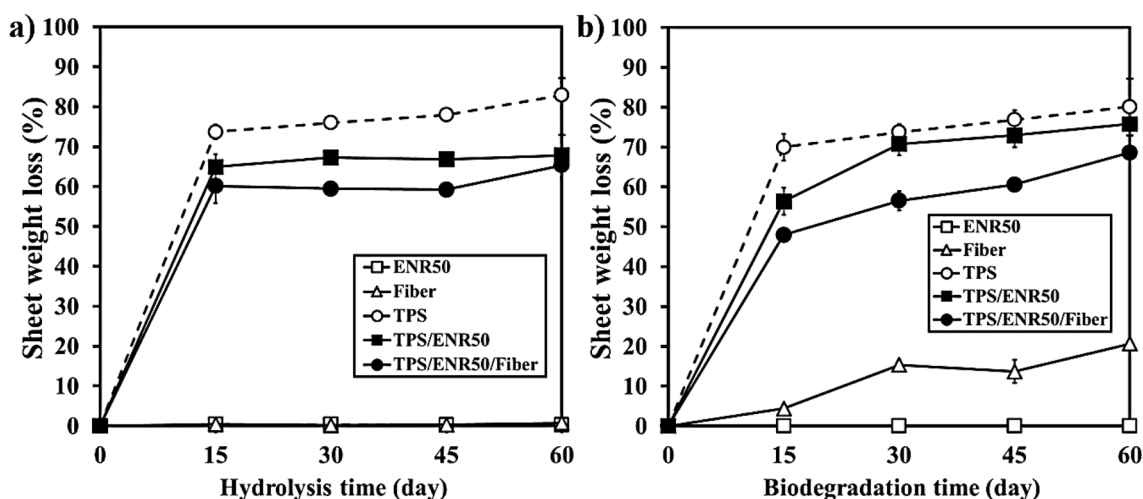


**Fig. 10** Weight loss percentages of TPS, TPS/ENR50 blend and TPS/ENR50/Fiber composite under (a) submerged condition and (b) soil burial exposure

dramatically increased in the first 15 days, then increased with slower biodegradation rates. Noticeably, the weight loss percentage increased for the TPS blend and composite and the fiber under soil burial. The change in the fiber weight loss percentage after soil exposure and the unchanged weight of the fiber under hydrolysis indicated that an enzymatic degradation occurred. As a positive control sample, cellulose-based fiber served as a reliable indicator. The pristine TPS degraded faster than the TPS/ENR50 and TPS/ENR50/fiber composites because the hydrophilic characteristic of TPS introduced enzymatic hydrolysis to accelerate biodegradation, the TPS molecular chain decomposes into starch, and the microorganisms assimilated this generated starch as a carbon source [40]. In addition, the combined use of ENR50 and fiber increased the stability of the composite over that of TPS and TPS/ENR50, resulting in a lower percentage of weight loss. The added ENR increased the TPS stability because ENR has a high hydrocarbon content with minimal ingredients that microbes might consume, and the chemical interaction between TPS and ENR lowers the biodegradation rate [14, 41]. The addition of fiber increased the degradation period of TPS/ENR50 because the high crystallinity and dense molecular structure of cellulose hindered enzymatic hydrolysis and microorganism activities in TPS, corresponded with Babaei [13].

To better understand the effects of the combination of ENR and fiber on TPS stability and degradation, a schematic diagram of the degradation of TPS, TPS/ENR, and TPS/ENR/fiber by hydrolysis and enzymatic hydrolysis is given in Fig. 8. Chemical hydrolysis is started by the moisture absorption of hydrophilic TPS (Fig. 11). Water molecules ( $H_2O$ ) attached to the TPS surface and then formed hydrogen bonds with the hydroxyl groups ( $-OH$ ) of the TPS

molecules. Small molecules of water are preferable to large molecules of plasticizer, so the plasticizer was replaced with  $H_2O$  [42]. Any interaction between the TPS and plasticizer was destroyed, as the microorganisms in the environment attached to the starch surface and released  $\alpha$ -amylase to degrade it into amylose, especially in amorphous regions of TPS [43]. After that, the amylose was assimilated by the microbes.

The effects of ENR and fiber on TPS stability and degradation are introduced in Fig. 11b. The interaction of ENR and TPS slowed down hydrolysis via covalent bonding between the epoxy group of ENR and the hydroxyl group of TPS. The strong interaction and hydrophobicity of ENR reduced the polarity of the TPS and hindered the hydrogen bonding between the TPS and water [33]. In addition, the use of ENR and fiber may not generate only covalent bonding between ENR–TPS but also hydrogen bonding of ENR–fiber and TPS–fiber (Fig. 11c). The strong interactions and insolubility of ENR combined with the high crystallinity and dense molecular structure of the cellulose fiber slowed down TPS hydrolysis and decreased the solubility [13]. The low rate of hydrolysis retarded enzyme production from microorganism activities, including amylases, cellulases, and glucosidases.

## Conclusions

The addition of ENR25 increased the tensile strength and elongation at break of the TPS more than that of TPS with added ENR50 or NR. Thus, the recommended content of ENR25 for blending with TPS is 20 wt%. Interestingly, the highest tensile strength, elongation at break, and tensile

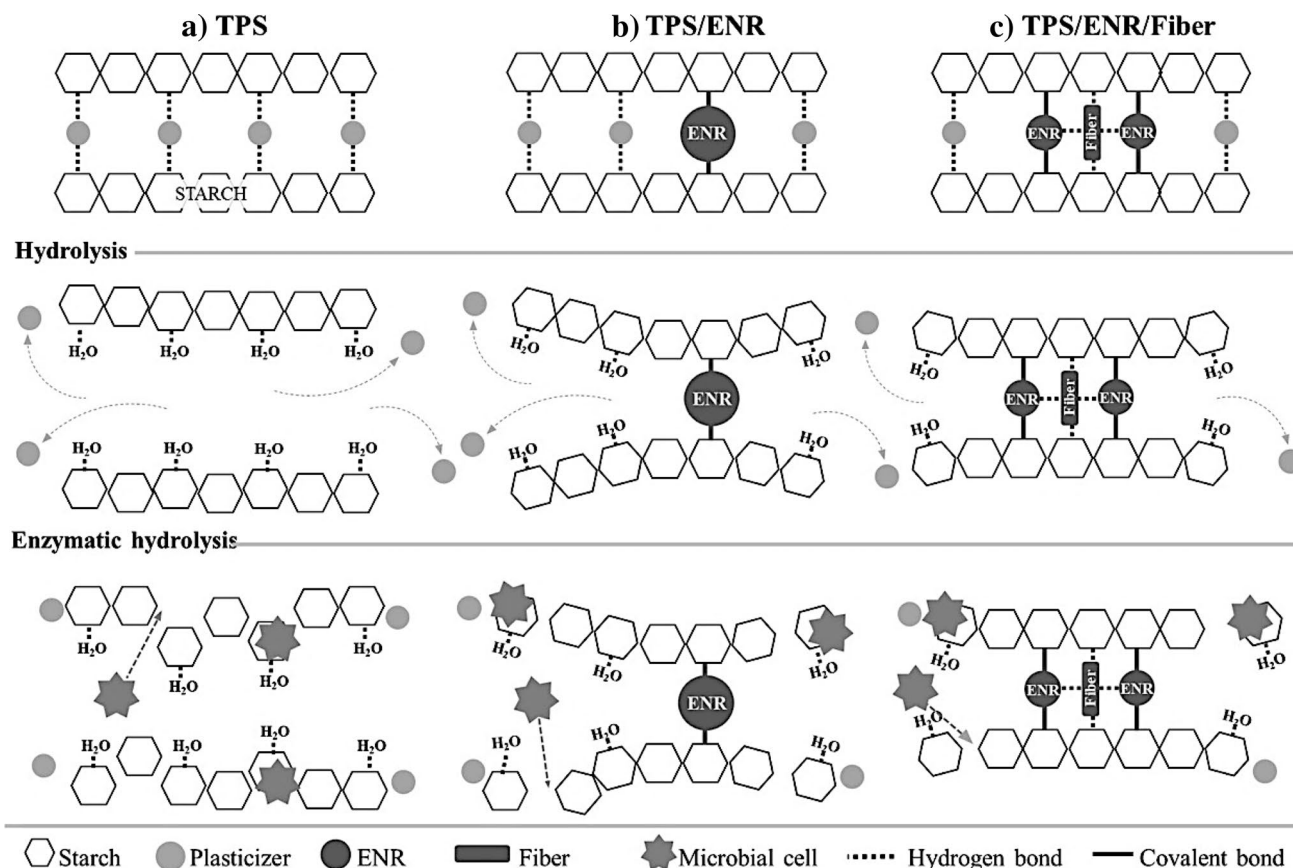


**Fig. 11** A schematic diagram of **a** TPS, **b** TPS/ENR and **c** TPS/ENR/Fiber degradation steps

modulus were found in TPS containing both ENR50 and fiber at the recommended amounts of 10% and 15 phr, respectively. Noticeably, the ENR50 had higher interacted to the TPS chain as a binder between the fiber and TPS than the ENR25, while the agglomeration of rubber phase reduced after incorporating fiber. The TPS/ENR50/fiber composite has higher thermal stability and water resistance than the other mixtures. The TPS with added ENR50 and fiber degraded slower and maintained its shape without disintegration under water and soil exposure. In summary, the recommended combination for improving the mechanical properties and stability is 10 wt % ENR50 and 15 phr fiber. This environmentally friendly materials could be use as seed tray, slow released fertilizer for agriculture applications.

**Authors Contribution** YB: Conceptualization, Methodology, Validation, Formal analysis, Investigation, Data Curation, Writing—Original Draft, Writing—Review & Editing, Visualization. PS: Methodology, Investigation, Resources. YN: Conceptualization, Methodology, Resources, Writing—Review & Editing, Supervision, Project administration, Funding acquisition.

**Funding** This work was funded by National Science, Research and Innovation Fund (NSRF) via the Program Management Unit for Human

Resources & Institutional Development, Research and Innovation [Grant No. B01F640031].

## Declarations

**Conflict of interest** The authors declare no competing interests.

## References

- Bangar SP, Whiteside WS, Ashogbon AO, Kumar M (2021) Recent advances in thermoplastic starches for food packaging: a review. *Food Packag Shelf Life* 30:100743. <https://doi.org/10.1016/j.fpsl.2021.100743>
- Hammache Y, Serier A, Chaoui S (2020) The effect of thermoplastic starch on the properties of polypropylene/high density polyethylene blend reinforced by nano-clay. *Mater Res Express* 7:025308. <https://doi.org/10.1088/2053-1591/ab7270>
- Noivoil N, Yoksan R (2021) Compatibility improvement of poly (lactic acid)/thermoplastic starch blown films using acetylated starch. *J Appl Polym Sci* 138:49675. <https://doi.org/10.1002/app.49675>
- Cai Z, Čadek D, Šmejkalová P, Kadeřábková A, Nová M, Kuta A (2021) The modification of properties of thermoplastic starch materials: combining potato starch with natural rubber and epoxidized natural rubber. *Mater Today Commun* 26:101912. <https://doi.org/10.1016/j.mtcomm.2020.101912>

5. Trabelsi S, Albouy PA, Rault J (2002) Stress-induced crystallization around a crack tip in natural rubber. *Macromolecules* 35:10054–10061. <https://doi.org/10.1021/ma021106c>
6. Hemsri S, Thongpin C, Somkid P, Sae-Arma S, Paiykaew A (2015) Improvement of toughness and water resistance of bioplastic based on wheat gluten using epoxidized natural rubber. *IOP Conf Ser: Mater Sci Eng* 87:012049. <https://doi.org/10.1088/1757-899X/87/1/012049>
7. Gelling IR (1985) Modification of natural rubber latex with peracetic acid. *Rubber Chem Technol* 58:86–96. <https://doi.org/10.5254/1.3536060>
8. Trovatti E, Carvalho AJF, Gandini A (2015) A new approach to blending starch with natural rubber. *Polym Int* 64:605–610. <https://doi.org/10.1002/pi.4808>
9. Jantanasakulwong K, Leksawasdi N, Seesuriyachan P, Wong-suriyasak S, Techapun C, Ougizawa T (2016) Reactive blending of thermoplastic starch, epoxidized natural rubber and chitosan. *Eur Polym J* 84:292–299. <https://doi.org/10.1016/j.eurpolymj.2016.09.035>
10. Gutiérrez TJ, Alvarez VA (2017) Cellulosic materials as natural fillers in starch-containing matrix-based films: a review. *Polym Bull* 74:2401–2430. <https://doi.org/10.1007/s00289-016-1814-0>
11. Heinze T, El Seoud OA, Koschella A (2018) Production and characteristics of cellulose from different sources. *Cellul Deriv*. [https://doi.org/10.1007/978-3-319-73168-1\\_1](https://doi.org/10.1007/978-3-319-73168-1_1)
12. de Farias JGG, Cavalcante RC, Canabarro BR, Viana HM, Scholz S, Simão RA (2017) Surface lignin removal on coir fibers by plasma treatment for improved adhesion in thermoplastic starch composites. *Carbohydr Polym* 165:429–436. <https://doi.org/10.1016/j.carbpol.2017.02.042>
13. Babaee M, Jonoobi M, Hamzeh Y, Ashori A (2015) Biodegradability and mechanical properties of reinforced starch nanocomposites using cellulose nanofibers. *Carbohydr Polym* 132:1–8. <https://doi.org/10.1016/j.carbpol.2015.06.043>
14. Pichaiyut S, Wisunthorn S, Thongpet C, Nakason C (2016) Novel ternary blends of natural rubber/linear low-density polyethylene/thermoplastic starch: influence of epoxide level of epoxidized natural rubber on blend properties. *Iran Polym J* 25:711–723. <https://doi.org/10.1007/s13726-016-0459-z>
15. Lee SY, Gan SN, Hassan A, Terakawa K, Hattori T, Ichikawa N, Choong DH (2011) Reactions between epoxidized natural rubber and palm oil-based alkyds at ambient temperature. *J Appl Polym Sci* 120:1503–1509. <https://doi.org/10.1002/app.33290>
16. Kahar AWM, Ismail H (2016) High-density polyethylene/natural rubber blends filled with thermoplastic tapioca starch: physical and isothermal crystallization kinetics study. *J Vinyl Addit Technol* 22:191–199. <https://doi.org/10.1002/vnl.21422>
17. The PL, Ishak ZM, Hashim AS, Karger-Kocsis J, Ishiaku US (2004) Effects of epoxidized natural rubber as a compatibilizer in melt compounded natural rubber–organoclay nanocomposites. *Eur Polym J* 40:2513–2521. <https://doi.org/10.1016/j.eurpolymj.2004.06.025>
18. Johnson T, Thomas S (2000) Effect of epoxidation on the transport behavior and mechanical properties of natural rubber. *Polymer* 41:7511–7522. [https://doi.org/10.1016/S0032-3861\(00\)00076-8](https://doi.org/10.1016/S0032-3861(00)00076-8)
19. Jaratrotkamjorn R, Khaokong C, Tanrattanakul V (2012) Toughness enhancement of poly (lactic acid) by melt blending with natural rubber. *J Appl Polym Sci* 124:5027–5036. <https://doi.org/10.1002/app.35617>
20. Esmaeili M, Pircheraghi G, Bagheri R (2017) Optimizing the mechanical and physical properties of thermoplastic starch via tuning the molecular microstructure through co-plasticization by sorbitol and glycerol. *Polym Int* 66:809–819. <https://doi.org/10.1002/pi.5319>
21. Carvalho AJFD, Job AE, Alves N, Curvelo AADS, Gandini A (2003) Thermoplastic starch/natural rubber blends. *Carbohydr Polym* 53:95–99. [https://doi.org/10.1016/S0144-8617\(03\)00005-5](https://doi.org/10.1016/S0144-8617(03)00005-5)
22. Pongtanayut K, Thongpin C, Santawitee O (2013) The effect of rubber on morphology, thermal properties and mechanical properties of PLA/NR and PLA/ENR blends. *Energy Procedia* 34:888–897. <https://doi.org/10.1016/j.egypro.2013.06.826>
23. Kaewtatip K, Thongmee J (2012) Studies on the structure and properties of thermoplastic starch/luffa fiber composites. *Mater Des* 40:314–318. <https://doi.org/10.1016/j.matdes.2012.03.053>
24. Fahrngruber B, Eichelter J, Erhäusl S, Seidl B, Wimmer R, Mundt N (2019) Potato-fiber modified thermoplastic starch: effects of fiber content on material properties and compound characteristics. *Eur Polym J* 111:170–217. <https://doi.org/10.1016/j.eurpolymj.2018.10.050>
25. Saetun V, Chiachun C, Riyajan SA, Kaewtatip K (2017) Green composites based on thermoplastic starch and rubber wood sawdust. *Polym Compos* 38:1063–1069. <https://doi.org/10.1002/pc.23669>
26. Jiang MP, Zhang JH, Wang YH, Ahmad I, Guo X, Cao LM, Huang J (2021) Covalent-bond-forming method to reinforce rubber with cellulose nanocrystal based on the thiol-ene click reaction. *Compos Commun* 27:100865. <https://doi.org/10.1016/j.coco.2021.100865>
27. Cao L, Huang J, Chen Y (2018) Dual cross-linked epoxidized natural rubber reinforced by tunicate cellulose nanocrystals with improved strength and extensibility. *ACS Sustain Chem Eng* 6:14802–14811. <https://doi.org/10.1021/acssuschemeng.8b03331>
28. Savadekar NR, Mhaske ST (2012) Synthesis of nano cellulose fibers and effect on thermoplastics starch based films. *Carbohydr Polym* 89:146–151. <https://doi.org/10.1016/j.carbpol.2012.02.063>
29. Faibunchan P, Nakaramontri Y, Chueangchayaphan W, Pichaiyut S, Kummerlöwe C, Vennemann N, Nakason C (2018) Novel biodegradable thermoplastic elastomer based on poly (butylene succinate) and epoxidized natural rubber simple blends. *J Polym Environ* 26:2867–2880. <https://doi.org/10.1007/s10924-017-1173-4>
30. Faibunchan P, Pichaiyut S, Kummerlöwe C, Vennemann N, Nakason C (2020) Green biodegradable thermoplastic natural rubber based on epoxidized natural rubber and poly (butylene succinate) blends: influence of blend proportions. *J Polym Environ* 28:1050–1106. <https://doi.org/10.1007/s10924-020-01655-5>
31. Zhou H, Long Y, Meng A, Li Q, Zhang Y (2015) Classification of municipal solid waste components for thermal conversion in waste-to-energy research. *Fuel* 145:151–157. <https://doi.org/10.1016/j.fuel.2014.12.015>
32. Cao X, Zhang J, Cen K, Chen F, Chen D, Li Y (2021) Investigation of the relevance between thermal degradation behavior and physicochemical property of cellulose under different torrefaction severities. *Biomass Bioenergy* 148:106061. <https://doi.org/10.1016/j.biombioe.2021.106061>
33. Zhang CW, Nair SS, Chen H, Yan N, Farnood R, Li FY (2020) Thermally stable, enhanced water barrier, high strength starch biocomposite reinforced with lignin containing cellulose nanofibrils. *Carbohydr Polym* 230:115626. <https://doi.org/10.1016/j.carbpol.2019.115626>
34. Alessandra L, Da Róza MDZ, Antonio ASC, Antonio JFC (2011) Thermoplastic starch modified during melt processing with organic acids: the effect of molar mass on thermal and mechanical properties. *Ind Crops Prod J* 33:152–215. <https://doi.org/10.1016/j.indcrop.2010.09.015>
35. Ab Wahab MK, Mohamad HS, Jayamani E, Ismail H, Wnuk I, Przybył A, Stachowiak T, Postawa P (2021) Effect of sago starch modifications on polystyrene/thermoplastic starch blends. *Materials* 14:2867. <https://doi.org/10.3390/ma14112867>
36. Abdul Wahab MK, Ismail H, Othman N (2012) Compatibilization effects of PE-g-MA on mechanical, thermal and swelling

- properties of high density polyethylene/natural rubber/thermoplastic tapioca starch blends. *Polym Plast Technol Eng* 51:298–303. <https://doi.org/10.1080/03602559.2011.639331>
37. Bondeson D, Syre P, Niska KO (2007) All cellulose nanocomposites produced by extrusion. *J Biobased Mater Bioenergy* 1:367–371. <https://doi.org/10.1166/jbmb.2007.011>
38. Ghanbari A, Tabarsa T, Ashori A, Shakeri A, Mashkour M (2018) Thermoplastic starch foamed composites reinforced with cellulose nanofibers: thermal and mechanical properties. *Carbohydr Polym* 197:305–311. <https://doi.org/10.1016/j.carbpol.2018.06.017>
39. Chamnanvachakit P, Prodpran T, Benjakul S, Prasarnpran S (2015) Use of epoxidized natural rubber (ENR) for property improvement of gelatin film, *Indian. J Sci Technol* 8:1–10. <https://doi.org/10.17485/ijst/2015/v8i36/54343>
40. Bootklad M, Kaewtatip K (2015) Biodegradability, mechanical, and thermal properties of thermoplastic starch/cuttlebone composites. *Polym Compos* 36:1401–1406. <https://doi.org/10.1002/pc.23046>
41. Aziana AH, Filza S, Roslim R, Fatimah Rubaizah MR (2021) Assessing biodegradability of epoxidized natural rubber latex. *J Rubber Res* 24:595–605. <https://doi.org/10.1007/s42464-021-00109-4>
42. Jantanasakulwong K, Homsaard N, Phengchan P, Rachtanapun P, Leksawasdi N, Phimolsiripol Y, Techapun C, Jantrawut P (2019) Effect of dip coating polymer solutions on properties of thermoplastic cassava starch. *Polymers* 11:1746. <https://doi.org/10.3390/polym11111746>
43. Polman EM, Gruter GJM, Parsons JR, Tietema A (2021) Comparison of the aerobic biodegradation of biopolymers and the corresponding bioplastics: a review. *Sci Total Environ* 753:141953. <https://doi.org/10.1016/j.scitotenv.2020.141953>

**Publisher's Note** Springer Nature remains neutral with regard to jurisdictional claims in published maps and institutional affiliations.

Springer Nature or its licensor (e.g. a society or other partner) holds exclusive rights to this article under a publishing agreement with the author(s) or other rightsholder(s); author self-archiving of the accepted manuscript version of this article is solely governed by the terms of such publishing agreement and applicable law.